

Quasi-lattice of qubits and multipartite entanglement

Hou Ian

Institute of Applied Physics and Materials Engineering, FST, University of Macau, Macau

Unlike atoms in a lattice, the spacings between neighboring qubits in a superconducting quantum circuit are mesoscopic and non-uniform. The strength of interaction between this quasi-lattice chain of qubits and a resonator mode in circuit transmission lines is inhomogeneous and geometrically dependent on the circuit layout. We propose a projection-deformation method to give analytically the eigenstates of the quasi-particle excitation that arise in the quasi-lattice. We further show that, during the quasi-particle excitation, the distribution of multi-photon resonances between the resonator photon and the quasi-lattice is determined by the degree the quasi-lattice is deformed from a normal lattice. The multi-photon resonances lead to simultaneous generation of GHZ-type and W -type of multipartite entanglement states of the qubits, which is enhanced by the inhomogeneous interaction. Comparing the concurrence and the 3-tangle generated, we find that the totally non-separable GHZ entanglement is specifically increased, up to two orders of magnitude.

PACS numbers: 42.50.Ct, 32.80.Qk, 85.25.-j

Introduction — Fabricated from Josephson junctions, superconducting qubits act like macroscopic analogues of two-level atoms in superconducting quantum circuits [1]. When coupled to a microwave field via a transmission line or coplanar waveguide resonator in the circuits, they exhibit equivalent circuit versions of atomic optical effects [2], such as lasing [3, 4], electromagnetically induced transparency [5, 6], and parametric amplification [7]. The qubit-resonator interaction, emulating the atom-field interaction, is also responsible for the generation of entanglements in superconducting circuits [8], granting superconducting quantum circuits a key role in solid-state quantum computation [9].

The entanglement is generated by coupling multiple qubits to a single resonator mode simultaneously, exciting the qubits in a synchronous fashion [10]. This multi-qubit coupling again mirrors that of atoms, for which the classical Dicke model or Tavis-Cummings (TC) model [11] is used. Therefore, much like the strong coupling between an atomic ensemble and an optical cavity field [12–15], that between a set of qubits and a circuit resonator mode also scales with \sqrt{N} where N is the number of qubits. However, superconducting qubits have major distinctions from real atoms: their macroscopic sizes and their artificiality, which renders the classical models irrelevant in many scenarios. To accommodate the analysis of the experiments to the classical models, the qubits have to be placed at the antinodes of the resonator mode [16] or the transmission line has to be stretched long to place all the qubits about the center [17].

In general scenarios, the macroscopic sizes of the qubits make the qubit-qubit interspacings comparable to the wavelength of the coupling resonator mode, resulting in an inhomogeneous coupling even when the interspacings are uniform. In addition, the artificial fabrications of the qubits cannot guarantee the uniformity of interspacings like that of an atomic lattice, resulting in a further complication in the inhomogeneous coupling. These two distinctions imply a chain of qubits in a superconducting quantum circuit is at the most a quasi-lattice and its mesoscopic nature is not fully captured by the classical models. To address this issue, we introduce here a projection-

deformation method to diagonalize the inhomogeneous interaction, whose preliminary model for uniformly spaced quasi-lattice was given in Ref. [18]. More importantly, how the inhomogeneous coupling would affect the entanglement generation is still unknown and we investigate this problem which would bear strong relevance to solid-state quantum information processing in this letter.

We first extend the diagonalization method to general non-uniform spacing cases through a modification to the deformation factor of the quasi-lattice. Then we find the collective quasi-particle excitation of the quasi-lattice through this deformation factor, which quantifies how much the quasi-lattice deviates from normal lattices and thus measures how asynchronous the qubits are excited to form the collective excitation. The asynchronous excitation avoids full inversion of the quasi-lattice and, following Dicke's notions, yields higher cooperation among the qubits. Consequently, the quasi-lattice receives higher probability in multi-photon resonances with the resonator, resulting in a more entangled state than it would be achievable in normal lattice settings.

To be more specific, it is found that not only the W -type, but also the GHZ-type of entanglement is generated during the multi-photon resonance processes, the latter of which is usually much harder to generate. Since these two types of entanglements are inequivalent to each other [19, 20], i.e. one cannot obtain one state from the other through local operations with classical communications (LOCC), the ability to generate both without complex quantum gate routines will benefit the development of quantum computers. Moreover, it was shown that the mechanism to generate W -states becomes faster when the TC-coupling is inhomogeneous [21], which verifies from another angle that inhomogeneous coupling facilitates quantum information processing. We also note that the discussion here applies equally well to other inhomogeneously coupled systems, such as electron spins [22].

Quasi-lattice — To identify the problem more clearly, we

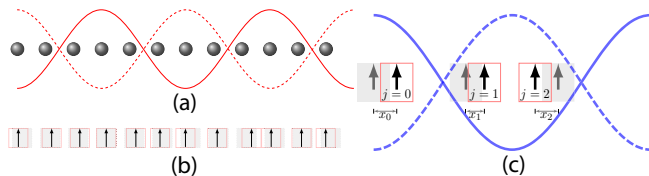


Figure 1: (color online) Illustrations of inhomogeneous interactions on a quasi-lattice. (a) Uniform lattice spacing L_q between atoms is comparable to the resonator wavelength λ_p (the case with $\ell = 1/3$ is illustrated). (b) Qubits have non-uniform spacing L_q in a mesoscopic quasi-lattice. Their positions (red boxes) are dislocated from the “equilibrium” coordinates j (gray shades in the background). (c) A 3-qubit quasi-lattice with $\ell = 2/3$ and position deviations x_0 , x_1 , and x_2 from equilibrium coordinates $j = 0, 1$, and 2 , respectively.

consider the following interaction Hamiltonian

$$H_{\text{int}} = \sum_{j=0}^{N-1} g_j (\sigma_{j,+} a + \sigma_{j,-} a^\dagger) \quad (1)$$

where $g_j \neq g_k$ for $j = k$ in general. In the equation, a denotes the annihilation operator for the cavity resonator mode and $\sigma_{j,+}$ the spin-up operator for the j -th atom or qubit. The non-rotating terms are discarded because we assume each g_j operates in the weak-coupling regime and N is not sufficiently large on the mesoscopic scale to warrant collective effects on the virtual photon processes.

To give an exact description of the inhomogeneous coupling strengths g_j , we consider two cases. First, each qubit has a uniform lattice spacing L_q to its neighboring qubits. The dipole-field coupling has an explicit sinusoidal dependence: $g_j = g \cos(j\pi\ell)$, as illustrated in Fig. 1(a), where the quasi-lattice is still uniformly spaced like normal lattices. The ratio $\ell = 2L_q/\lambda_p$ of L_q with respect to the wavelength λ_p of the resonator mode is a fixed fraction (the factor 2 is added to simplify the mathematical expressions given below). Using the terminology of solid-state theory, we can regard ℓ as the relative lattice spacing and j as the dimensionless integer coordinate in units of L_q for the equilibrium positions of the qubits.

Secondly, even though the qubits do not vibrate as real atoms do, the qubits can be dislocated from their theoretical equilibrium positions due to fabrication. Since this dislocation is unpredictable, we consider the dimensionless deviation x_j of each qubit from its respective equilibrium point as a random variable whose value is small compared to the coordinate j . The coupling factor that results is of the form $\cos(j+x_j)\pi\ell$, shown in Fig. 1(b) with the same number of lattice points in (a). Fig. 1(c) gives a detailed illustration of the position dependence of g_j on ℓ for a $N = 3, \ell = 2/3$ quasi-lattice. We see that different sets of qubits will be driven at different Rabi frequencies by either variably spacing the qubits or controlling the harmonic modes in the transmission line resonator.

If each qubit is driven at the same rate by the resonator, neighboring qubits will become fully excited at equal rate. Spontaneous radiation rates of all the qubits reach maximum

synchronously in the quasi-lattice. Consequently, the probability of simultaneous absorption of multiple photons is low. In contrast, if the quasi-lattice is non-uniform with the qubits driven at inhomogeneous rates, neighboring qubits will become fully excited asynchronously. That means while some qubit is spontaneously radiating photons, other qubits which are not totally excited have high probability to either absorb the resonator photons or reabsorb the radiated photons. This circumstance leads to a high probability of multi-photon resonance of the resonator mode with the ground state of the quasi-lattice.

Quasi-particles — To verify that the non-uniform coupling indeed increases the probability of multi-photon resonance in the qubits, we can examine the eigenspectrum of the collective quasi-particle excitations in the quasi-lattice. For such collective excitations, each quantized energy level does not correspond to the energy level of the excited state of a particular qubit, but to a delocalized probability excitation level of the quasi-lattice as a whole.

To give analytical expressions for the eigenstates of the quasi-particles, we write Eq. (1) as $H_{\text{int}} = g(S_+ a + S_- a^\dagger)$ where $g = \max(\{g_j\})$. The operators $S_\pm = \sum_j \eta_j \sigma_{j,\pm}$ with $\eta_j = g_j/g$ can be regarded as the ladder operators on the total spin angular momentum. Correspondingly, the free Hamiltonian can be written as $H_0 = \omega_q S_z + \omega_0 a^\dagger a$, where $S_z = \sum_j \sigma_{j,z}$ accounts for the spin magnetic moment. ω_q and ω_0 are, respectively, the level spacing for all qubits and the frequency for the resonator mode.

In order to make the interaction block-diagonalizable as that in TC-model, the set of operators $\{S_\pm, S_z\}$ must conform to a $SU(2)$ Lie algebra. Nonetheless, since $[S_+, S_-] \neq 2S_z$ because of the non-uniform coupling in the quasi-lattice, we approximate the set as a deformed algebra by projecting the commutator into the $SU(2)$ group manifold through a trace over the Hilbert space spanned by the quasi-lattice. This method associates with the deformation of the Bloch sphere S^2 , which is the two-dimensional projection of the 3-sphere S^3 isomorphic to $SU(2)$, into an ellipsoid and we call this method the projection-deformation (PD) method. The degree of elongation of the resulting ellipsoid from the original 2-sphere is the deformation factor $\tilde{f} = \sum_{j=0}^N \eta_j^2 / N$, where the $\eta_j(\ell, x_j)$ are functions of both the relative spacing ℓ and the random variables x_j .

The deformation factor \tilde{f} measures how the inhomogeneously excited spin operators $\{S_\pm, S_z\}$ differ from a standard $SU(2)$ algebra and serves thus a measure of the degree the quasi-lattice resembles a normal lattice. When the random variables x_j vanish for uniformly spaced quasi-lattices, \tilde{f} is a number that depends on ℓ and N only. When the quasi-lattice is non-uniformly spaced, \tilde{f} is itself a random variable with zero mean. Considering the randomness is introduced by the fabrication technologies, we take the x_j as identical, independent, normally distributed variables with variance σ^2 . Then the deformation factor can be given as a numerical factor can be given as the expectation value of \tilde{f} , i.e.

$$f = \mathbb{E}(\tilde{f}) = \frac{1 + (\pi\ell\sigma)^2}{2} + \frac{1 - (\pi\ell\sigma)^2}{4N} \left(1 + \frac{\sin(2N - 1)\pi\ell}{\sin\pi\ell} \right) \quad (2)$$

through Hilbert-Schmidt norm [18], where averaging over the quasi-lattice $[\frac{1}{N} \sum_j]$ is taken to be equivalent to taking discrete expected values for sufficiently large N . When the variance is omitted, f falls back to the special case for uniformly spaced quasi-lattices.

After the PD process of $SU(2)$, the diagonalized Hamiltonian in Eq. (1) has eigenvalues

$$E_u = \omega_q u + \varepsilon \quad (3)$$

for a quasi-particle ‘‘excitation’’ number $u = n + m$, which is distributed among the photon count n from the resonator and the spin moment m from the quasi-lattice. Since we have adopted the angular momentum model, u can take either integer or half-integer values greater than $(-N/2)$. The second term ε accounts for the qubit-photon detuning $\Delta\omega = \omega_0 - \omega_q$ and the lattice-photon interaction with maximum coupling strength g . Hence, it is a function of both of these two numbers. At resonance with $\Delta\omega = 0$, this energy ε will be a multiple of g only.

Without ε , the eigenstates for each E_u has a $(u + r + 1)$ -fold degeneracy distributed among different combinations of n and m : $|u, r\rangle = \sum_{n=0}^{u+r} c_n |n\rangle \otimes |r, m\rangle$, where r is the total spin number for N qubits. That means, the finite interaction splits each degeneracy into finer levels with splitting ε , analogous to ac-Stark shifts to an atom. Both this splitting ε and the coefficients c_n are determined *a posteriori* by a recursive relation

$$c_n = \frac{\varepsilon - \Delta\omega(n-1)}{g\alpha_{r,m}\sqrt{n\tilde{f}}} c_{n-1} - \sqrt{\frac{n-1}{n}} \frac{\alpha_{r,m+1}}{\alpha_{r,m}} c_{n-2} \quad (4)$$

with initial conditions $c_{u+r+1} = c_{-1} = 0$. In the relation, $\alpha_{r,m} = \sqrt{(r-m)(r+m+1)}$ are the off-diagonal elements of the ladder operators. The initial value c_0 can take arbitrary value since the subsequent coefficients are all multiples of c_0 , hence it can be regarded as a constant arbitrarily chosen for normalization. The analytical expressions for c_n and ε can be found by treating Eq. (4) as a difference equation [18]. The coefficients c_n , which represent the probability amplitudes of different mixed resonant states between the quasi-lattice and the resonator photon, are not only determined by the off-diagonal transition elements, but are also determined by the deformation factor f . The latter is thus a structure parameter of the quasi-lattice that decides the form each photon is transferred to all the qubits, affecting how entanglement is generated among the qubits.

Multi-photon resonances — To generate entanglement of the qubits, a photon is brought into resonance with the quasi-lattice. In the case of superconducting quantum circuits, this is achieved by sending a pulse signal into the qubit such that the qubit level spacing is tuned in-resonance with the waveguide

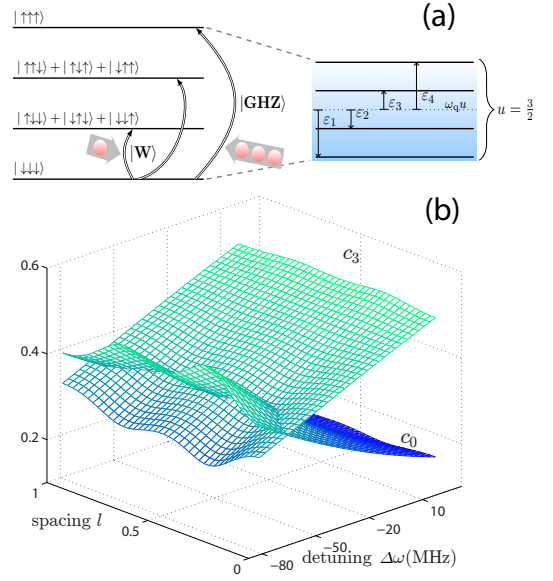


Figure 2: (color online) (a) The level diagram of a 3-qubit quasi-lattice, with the ground state resonant with multiple photons, forming two classes of entanglement states ($|GHZ\rangle$ and $|W\rangle$ states). The energy levels are effectively dressed into a cluster of states of the same ‘‘excitation’’ number $3/2$, split by shifts $\varepsilon_{1,2,3,4}$ due to the lattice-photon interaction. (b) The distribution of the normalized coefficients c_0 of the ground state and c_3 of the excited state versus the relative qubit spacing and the detuning for the clustered state $|u = \frac{3}{2}\rangle$.

resonator [10]. Close to the resonator-qubit avoided-crossing point, the resonator mode dresses the quasi-lattice states into a series of clusters of states, grouped by the value of u . For the 3-qubit quasi-lattice in Fig. 1(c), this dressing process is illustrated in Fig. 2(a), for which the clustered $u = \frac{3}{2}$ excited level is split into four sublevels for the four values of the splitting ε .

During dressing, the excitation number u shared between the photon Fock states and the quasi-lattice angular-momentum states is conserved. The fixed u permits both single-photon resonance (between $|n = u + r\rangle$ and $|n = u + r - 1\rangle$) and multi-photon resonances (between $|n = u + r\rangle$ and $|n = u - m\rangle$ where $m > -r + 1$). Simultaneous occurrences of different resonance processes then generate entanglement states of inequivalent classes, each with a different probability. We take the 3-qubit quasi-lattice in Fig. 1(c) again as an example. The quasi-lattice at ground state $|\frac{3}{2}, -\frac{3}{2}\rangle$ can be resonant with both $|\frac{3}{2}, \frac{3}{2}\rangle$ through a triple-photon process to generate the $|GHZ\rangle$ state and $|\frac{3}{2}, -\frac{1}{2}\rangle$ through a single-photon process to generate the $|W\rangle$ state. These two processes are illustrated on the left side of Fig. 2(a). The states of the qubits in $|\frac{3}{2}, \frac{1}{2}\rangle$ is equivalent to those of $|\frac{3}{2}, -\frac{1}{2}\rangle$ up to a LOCC operation, so the $|W\rangle$ state can also be generated through a double-photon resonance with the quasi-lattice ground state.

To determine how asynchronous excitations of the qubits actually benefit the generation of $|GHZ\rangle$ state through inho-

mogeneous coupling in the 3-qubit case, we calculate two coefficients c_0 and c_3 for the clustered dressed state $|u = \frac{3}{2}\rangle$, where they associate respectively with the eigenstates $|\uparrow\uparrow\uparrow\rangle$ and $|\downarrow\downarrow\downarrow\rangle$ of the $|\text{GHZ}\rangle$ state. The analytical solution to the two coefficients is subject to a common normalizing factor and their ratio can be compactly written as

$$\frac{c_0}{c_3} = \frac{6\sqrt{6}g^3f^{3/2}}{\varepsilon(\varepsilon - \Delta\omega)(\varepsilon - 2\Delta\omega) - (11\varepsilon - 6\Delta\omega)g^2f}. \quad (5)$$

Their numerical solutions for the highest split state of ε are plotted in Fig. 2(b) against the relative spacing ℓ on one axis and against the detuning $\Delta\omega$ on the other, using the experimental data given in Ref. [16].

We observe that at exact qubit-photon resonance or positive detuning, the coefficient c_0 for the all spin-up state is close to zero, meaning the probability of triple-photon resonance is low. In the range of negative detuning, which is the normal case for ω_0 is usually less than ω_q , c_0 starts to increase while the c_3 for the all spin-down state correspondingly decreases. The effect of the inhomogeneous coupling is reflected by the deformation factor f in Eq. (5), where the ratio can be expanded as a polynomial with roots indicating locations of extrema. The numerical solution given in Fig. 2(b) shows that c_0 obtains maximum at about $\ell \approx 0.3$ and $\ell \approx 0.7$, both numbers implying irregular spacings. This verifies our prediction that irregularity of the qubit spacings triggers asynchronous excitation of the qubits and increases the chance of multi-photon absorptions.

Multipartite entanglement— The entanglement among the three qubits that results from the multi-photon resonances also increases. Figure 3(a) plots the tripartite concurrence of pure state entanglement as a function of ℓ for three detuning values of $\Delta\omega$, using the definition given by Carvalho *et al.* [23] that generalizes the original bipartite concurrence given by Wootters [24]. Other parameters are set to the same values of those used in Fig. 2(b).

For the three values of detunings, the concurrences are all close to the maximum attainable value of 1.25, showing that the resonance between the quasi-lattice and the resonator photon generates highly entangled states among the qubits. It is particularly noticeable that the concurrence peaks at the same values of ℓ as those for the coefficient c_0 , showing that multi-photon absorptions facilitated by inhomogeneity also assist entanglement generation.

Since the absorbed photon does not discriminate the individual qubits, in other words, one exciton-polariton state of the quasi-lattice has equal probability of excited levels in any one of the three qubits, the entanglement generated is symmetrically distributed among all three qubits. Therefore, the probability of generating $|\text{GHZ}\rangle$ entangled state, which requires excitation of all three qubits at the same time, is greatly increased. To show this, we use the metric 3-tangle introduced by Coffman *et al.* [25] as it quantifies the three-party total non-separability of quantum states while concurrence accounts for both partial and total non-separabilities. To be exact, 3-tangle

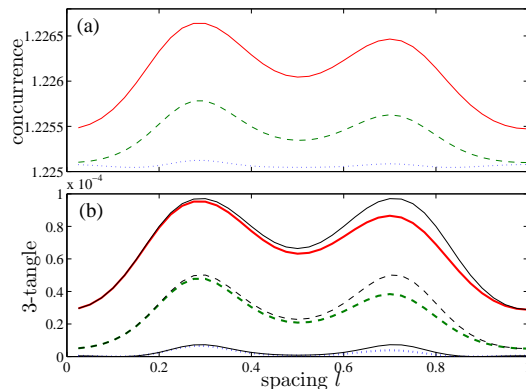


Figure 3: (color online) Tripartite entanglements measured in two metrics: (a) the tripartite concurrence and (b) the 3-tangle, at three values of detuning $\Delta\omega = 66\text{MHz}$ (red solid), $\Delta\omega = 92\text{MHz}$ (green dashed), and $\Delta\omega = 117\text{MHz}$ (blue dotted). The black solid lines in (b) are plotted with variance σ set to zero to indicate comparable uniform spacing cases.

is non-zero only for $|\text{GHZ}\rangle$ state and zero for $|W\rangle$ and other states [19, 26].

Figure 3(b) plots 3-tangle for the same three detunings and similar trends of variation as those in Fig. 3(a) are visible. Though the inhomogeneity does not contribute a dramatic increase in concurrence, its contribution to 3-tangle is apparent. For example, for $\Delta\omega = 92\text{MHz}$, 3-tangle is close to zero when the quasi-lattice is uniform at the two ends of abscissa; whereas at the $\ell = 0.3$ peak, the increase in 3-tangle is about 94-fold. As a comparison, the same cases but with variance σ set to zero are plotted in solid black in Fig. 3(b). We note that 3-tangle obtains its maximal value when the qubit spacings are set uniform. The non-uniformity in spacing captured by σ slightly reduces the entanglement but endows an asymmetric dependence on ℓ about the middle $\ell = 1/2$ point. This asymmetry coincides with our expectation that the disorder introduced by the non-uniform spacing further complexifies how the qubits are asynchronously excited. Nonetheless, this disorder does not deter the fact that the enhancement in entanglement goes mainly to the totally non-separable $|\text{GHZ}\rangle$ state.

The author thanks X. G. Wang, Q. Ai, S. Ashhab, and E. Lucero for stimulating discussion. The research is supported by UM under grant SRG003-FST12-IH and FDCT of Macau under grant 013/2013/A1.

-
- [1] A. Blais, R.-S. Huang, A. Wallraff, S. M. Girvin, and R. J. Schoelkopf, Phys. Rev. A **69**, 062320 (2004).
 - [2] J. Q. You and F. Nori, Nature **474**, 589 (2011).
 - [3] S. Ashhab, J. R. Johansson, A. M. Zagoskin, and F. Nori, New J. Phys. **11**, 023030 (2009).
 - [4] S. André, V. Brosco, M. Marthaler, A. Shnirman, and G. Schön, Phys. Scr. **2009**, 014016 (2009).
 - [5] H. Ian, Y. Liu, and F. Nori, Phys. Rev. A **81**, 063823 (2010).

- [6] J. Joo, J. Bourassa, A. Blais, and B. C. Sanders, *Phys. Rev. Lett.* **105**, 073601 (2010).
- [7] M. A. Castellanos-Beltran and K. W. Lehnert, *Appl. Phys. Lett.* **91**, 083509 (2007).
- [8] C. Eichler, C. Lang, J. M. Fink, J. Govenius, S. Filipp, and A. Wallraff, *Phys. Rev. Lett.* **109**, 240501 (2012).
- [9] M. Mariani, H. Wang, T. Yamamoto, M. Neeley, R. C. Bialczak, Y. Chen, M. Lenander, E. Lucero, A. D. O'Connell, D. Sank, M. Weides, J. Wenner, Y. Yin, J. Zhao, A. N. Korotkov, A. N. Cleland, and J. M. Martinis, *Science* **334**, 61 (2011).
- [10] E. Lucero, R. Barends, Y. Chen, J. Kelly, M. Mariani, A. Megrant, P. O'Malley, D. Sank, A. Vainsencher, J. Wenner, T. White, Y. Yin, A. N. Cleland, and J. M. Martinis, *Nat. Phys.* **8**, 719 (2012).
- [11] M. Tavis and F. W. Cummings, *Phys. Rev.* **170**, 379 (1968).
- [12] F. Brennecke, T. Donner, S. Ritter, T. Bourdel, M. Köhl, and T. Esslinger, *Nature* **450**, 268 (2007).
- [13] Y. Colombe, T. Steinmetz, G. Dubois, F. Linke, D. Hunger, and J. Reichel, *Nature* **450**, 272 (2007).
- [14] H. Ian, Z. R. Gong, Y. Liu, C. P. Sun, and F. Nori, *Phys. Rev. A* **78**, 013824 (2008).
- [15] D. Hunger, S. Camerer, T. W. Hänsch, D. König, J. P. Kotthaus, J. Reichel, and P. Treutlein, *Phys. Rev. Lett.* **104**, 143002 (2010).
- [16] J. M. Fink, R. Bianchetti, M. Baur, M. Göppl, L. Steffen, S. Filipp, P. J. Leek, A. Blais, and A. Wallraff, *Phys. Rev. Lett.* **103**, 083601 (2009).
- [17] P. Macha, G. Oelsner, J.-M. Reiner, M. Marthaler, S. André, G. Schön, U. Huebner, H.-G. Meyer, E. Il'ichev, and A. V. Ustinov, arXiv: 1309.5268 (2013).
- [18] H. Ian, Y. Liu, and F. Nori, *Phys. Rev. A* **85**, 053833 (2012).
- [19] W. Dür, G. Vidal, and J. I. Cirac, *Phys. Rev. A* **62**, 062314 (2000).
- [20] C. H. Bennett, S. Popescu, D. Rohrlich, J. A. Smolin, and A. V. Thapliyal, *Phys. Rev. A* **63**, 012307 (2000).
- [21] C. E. López, F. Lastra, G. Romero, E. Solano, and J. C. Retamal, *Phys. Rev. A* **85**, 032319 (2012).
- [22] J. Schliemann, A. V. Khaetskii, and D. Loss, *Phys. Rev. B* **66**, 245303 (2002).
- [23] A. R. R. Carvalho, F. Mintert, and A. Buchleitner, *Phys. Rev. Lett.* **93**, 230501 (2004).
- [24] W. K. Wootters, *Phys. Rev. Lett.* **80**, 2245 (1998).
- [25] V. Coffman, J. Kundu, and W. K. Wootters, *Phys. Rev. A* **61**, 052306 (2000).
- [26] R. Lohmayer, A. Osterloh, J. Siewert, and A. Uhlmann, *Phys. Rev. Lett.* **97**, 260502 (2006).